NASA/TM—2019-220377 AIAA–2019–4165

NEXT Ion Propulsion System Risk Mitigation Tests in Support of the Double Asteroid Redirection Test Mission

Robert E. Thomas and Michael J. Patterson
Glenn Research Center, Cleveland, Ohio

Mark W. Crofton
The Aerospace Corporation, El Segundo, California

Jeremy W. John
Johns Hopkins University Applied Physics Laboratory, Laurel, Maryland

November 2019

NASA STI Program . . . in Profile

Since its founding, NASA has been dedicated to the advancement of aeronautics and space science. The NASA Scientific and Technical Information (STI) Program plays a key part in helping NASA maintain this important role.

The NASA STI Program operates under the auspices of the Agency Chief Information Officer. It collects, organizes, provides for archiving, and disseminates NASA's STI. The NASA STI Program provides access to the NASA Technical Report Server—Registered (NTRS Reg) and NASA Technical Report Server—Public (NTRS) thus providing one of the largest collections of aeronautical and space science STI in the world. Results are published in both non-NASA channels and by NASA in the NASA STI Report Series, which includes the following report types:

- TECHNICAL PUBLICATION. Reports of completed research or a major significant phase of research that present the results of NASA programs and include extensive data or theoretical analysis. Includes compilations of significant scientific and technical data and information deemed to be of continuing reference value. NASA counter-part of peer-reviewed formal professional papers, but has less stringent limitations on manuscript length and extent of graphic presentations.

- TECHNICAL MEMORANDUM. Scientific and technical findings that are preliminary or of specialized interest, e.g., "quick-release" reports, working papers, and bibliographies that contain minimal annotation. Does not contain extensive analysis.

- CONTRACTOR REPORT. Scientific and technical findings by NASA-sponsored contractors and grantees.

- CONFERENCE PUBLICATION. Collected papers from scientific and technical conferences, symposia, seminars, or other meetings sponsored or co-sponsored by NASA.

- SPECIAL PUBLICATION. Scientific, technical, or historical information from NASA programs, projects, and missions, often concerned with subjects having substantial public interest.

- TECHNICAL TRANSLATION. English-language translations of foreign scientific and technical material pertinent to NASA's mission.

For more information about the NASA STI program, see the following:

- Access the NASA STI program home page at http://www.sti.nasa.gov

- E-mail your question to help@sti.nasa.gov

- Fax your question to the NASA STI Information Desk at 757-864-6500

- Telephone the NASA STI Information Desk at 757-864-9658

- Write to:
  NASA STI Program
  Mail Stop 148
  NASA Langley Research Center
  Hampton, VA 23681-2199

NASA/TM—2019-220377 AIAA–2019–4165

NEXT Ion Propulsion System Risk Mitigation Tests in Support of the Double Asteroid Redirection Test Mission

Robert E. Thomas and Michael J. Patterson
Glenn Research Center, Cleveland, Ohio

Mark W. Crofton
The Aerospace Corporation, El Segundo, California

Jeremy W. John
Johns Hopkins University Applied Physics Laboratory, Laurel, Maryland

Prepared for the
Propulsion and Energy Forum and Exposition
sponsored by the American Institute of Aeronautics and Astronautics
Indianapolis, Indiana, August 19–22, 2019

National Aeronautics and
Space Administration

Glenn Research Center
Cleveland, Ohio 44135

November 2019

Acknowledgments

The authors thank Kevin McCormick, Byron Zeigler, and Mike Worshum for their support with test preparations and set-up.

Level of Review: This material has been technically reviewed by technical management.

Available from

NASA STI Program
Mail Stop 148
NASA Langley Research Center
Hampton, VA 23681-2199

National Technical Information Service
5285 Port Royal Road
Springfield, VA 22161
703-605-6000

This report is available in electronic form at http://www.sti.nasa.gov/ and http://ntrs.nasa.gov/

NEXT Ion Propulsion System Risk Mitigation Tests in Support of the Double Asteroid Redirection Test Mission

Robert E. Thomas and Michael J. Patterson
National Aeronautics and Space Administration
Glenn Research Center
Cleveland, Ohio 44135

Mark W. Crofton
The Aerospace Corporation
El Segundo, California 90245

Jeremy W. John
Johns Hopkins University Applied Physics Laboratory
Laurel, Maryland 20723

Abstract

Risk mitigation tests have been conducted by the NASA Glenn Research Center and The Aerospace Corporation in support of the DART Mission. The tests focused on NEXT performance characterizations intended to ensure its operations and characteristics are compatible with the DART mission operations, and to assist in the definition of the propulsion system. Tests were performed at the Aerospace Corporation and they involved: flow sensitivity-analyses, steady-state performance characterizations, and measurements of thruster erosion. The tests also involved defining, demonstrating, verifying, and evaluating the start-up sequences and a beam current regulation algorithm consistent with DART mission requirements. It was found that NEXT thruster operations are compatible with the proposed relaxation of flow control ranges for ignition and for steady-state operation.

I. Nomenclature

g	=	gravitational constant, m/s^2
I_{sp}	=	specific impulse, s
J_a	=	accelerator current, A
J_b	=	beam current, A
J_d	=	discharge current, A
m_i	=	ion mass, kg
m_p	=	propellant mass, kg
q	=	ion charge state
T	=	thrust, N
V_b	=	beam voltage, V
V_g	=	coupling voltage, V
V_d	=	discharge voltage, V
α	=	doubly ionized thrust correction factor
β	=	divergence thrust correction factor
η_u	=	propellant utilization efficiency

II. Introduction

NASA's Double Asteroid Redirection Test (DART) will be the first demonstration of the kinetic impact technique to change the motion of an asteroid in space. The DART mission is led by Johns Hopkins University Applied Physics Laboratory (APL). The DART spacecraft will utilize the NASA Evolutionary Xenon Thruster (NEXT) solar electric propulsion system during flight operations. NEXT is the next generation system, a natural progression in gridded ion thruster technology from that implemented on the Deep-Space one and Dawn missions, developed at NASA's Glenn Research Center (GRC) in Cleveland, Ohio.[1-2] By utilizing electric propulsion, DART is able reduce the amount of hydrazine required for attitude control maneuvers and gain flexibility in mission operations.

The NEXT ion propulsion system has been under development since the early 2000s. Substantial progress has been made on the system, including performance, environmental, and system integration testing of engineering- and prototype-model (EM and PM) hardware, and lifetime assessment through both analysis and testing.[3-7] In 2015 NASA partnered with Aerojet-Rocketdyne and subcontractor ZIN Technologies to manufacture two thrusters and two power processing units (PPUs) for use on future NASA missions. This ongoing effort is called the NEXT-Commercial (NEXT-C) project. The approach of the project has been to address known issues with the PPU and thruster designs, meet any updates to the system requirements, and make design changes that reduce cost while maintaining the validity of the testing to date.[8-9] The first NEXT-C propulsion string will be delivered to APL for use on DART, while the second string is being reserved as a backup for the mission.

While Aerojet-Rocketdyne is contracted by GRC to deliver NEXT-C flight hardware, additional tests and analyses were required to support APL's definition and implementation of a NEXT-C ion propulsion system for DART. These tests and analyses included: Phase 1 testing, preceding the DART mission Preliminary Design Review, focusing on thruster operations; and Phase 2 testing, preceding the DART mission Critical Design Review (CDR), focusing on system-level demonstrations. The following section outlines the tests that have been conducted.

A. Test Sequence Definition

DART risk mitigation testing was conducted by GRC at The Aerospace Corporation with collaboration from APL. The Aerospace Corp. was under contract with GRC as both the test venue, and the executing organization with respect to plume diagnostics. The tests focused on NEXT performance characterizations intended to ensure its operations and characteristics are compatible with the DART mission Concept-of-Operations (CONOPS), and to assist in the definition of the propulsion system. The Phase 1 tests included: (a) detailed characterizations of mission-specific throttle levels; (b) definition of mission-specific profiles including thruster start-up and beam-control algorithms.

(a) Detailed characterizations of the mission-specific throttle levels – DART mission operation is intended to be primarily at NEXT Throttle Level 28 (TL28), about 3,220 W thruster input power at 3,140 seconds specific impulse yielding a thrust level of 137 mN. It should be noted that during the NEXT Phase II development program, all ground tests were conducted using xenon feed systems with a maximum flow tolerance of +/-3%. Given that NEXT will nominally operate at a single operating point during the DART mission, APL opted to use commercial-off-the-shelf flow restrictors to provide propellant to the engine. While this potentially simplifies the xenon feed system, it came at the expense of a) reduced flow accuracy; and b) the inability to throttle flows, which is typically done during NEXT startup operations. The risk reduction tests therefore focused on characterizing the engine during start-up and steady-state operations within the tolerance bands of the chosen flow restrictors. The tests involved: flow sensitivity-analyses; steady-state performance characterizations; and measurements of thruster erosion. The performance and erosion data were used to refine lifetime estimates. The sensitivity-analyses subtask evaluated NEXT thruster sensitivity at TL28, and other selected power levels adjacent to TL28. The evaluation involved dynamic control of individual NEXT thruster input parameters, documenting thruster response, operating margins, and beam charge state.

The steady-state performance subtask evaluated the NEXT thruster performance at TL28, and other selected power levels near TL28. The goals of this subtask were to verify thruster performance against that documented in NASA's standard Throttle Table 11.1, characterize the plume expansion, and in particular document the presence of energetic high-angle ions which may be of relevance to spacecraft integration. The results of these tests were used

to: refine performance measurements at DART mission conditions; document the thruster plume at the specified throttle levels with sufficient fidelity and spatial extent to provide validation data for modeling/simulation of the thruster plume, and; generate sufficient data to develop a DART-specific Throttle Table which may be necessary to support the definition of throttle level increments between NEXT TL29-and-ETL2.7A – power-throttling, at fixed propellant flow rates, from about 3,640 W down to about 2,990 W.

The life/erosion subtask evaluated the NEXT thruster erosion signatures at TL28 and other selected power levels. By thruster erosion signatures, the primary emphasis is the erosion of molybdenum from the thruster ion optics accelerator electrode due to both direct-energetic ion erosion and charge-exchange ion erosion – at the specified throttle levels, applying spatially-resolved Laser Induced Fluorescence (LIF) spectroscopy. A collimated quartz crystal microbalance probe and witness samples were also utilized to obtain information about sputter erosion products and net deposition at specific throttle levels. These data were used to verify and refine: knowledge of thruster surface erosion rates; thruster eroded-product deposition rates; and thruster life time projections at the proposed DART flight throttle levels. The results of the Phase 1 diagnostic tests are presented in Refs. [10-11], and will be referenced as necessary within this document.

(b) Definition and Verification of Mission Specific Algorithms – These tests involved defining, demonstrating, verifying, and evaluating the startup sequence for DART at TL28, and other selected intermediate power levels, over a range of anticipated DART initial thermal conditions. Measurements of the thrust vector and thrust vector stability, during the startup transient, were also documented. These data were used to: provide data to define the flight XFS flow control requirements and commands, and the PPU commands and sequences; and provide data for thruster gimbal control. Outcomes of this test include: verifying startup sequences at all anticipated initial conditions (throttle level, and thermal); and characterizing the thrust vector and thrust vector stability during the startup transient. The tests also involved defining, demonstrating, verifying, and evaluating the Beam Current Regulation Algorithm for DART. The goals of these tests were to define, demonstrate, and verify the system algorithms at the thruster-level, consistent with the DART CONOPS and thrust control requirements.

This manuscript describes the Phase 1 and 2 risk mitigation tests performed in support of the DART mission. A synopsis of key findings and associated implications relative to the DART IPS and CONOPS are provided for each test, along with reference to companion publications which provide more detailed probe diagnostic data.

III. Test Set Up

Tests were conducted using the engineering model 4 (EM4) thruster, which was manufactured at NASA GRC. The NEXT EM discharge chamber utilizes a hollow cathode and semi-conic chamber with a ring cusp magnetic circuit for electron containment. The thruster employs a neutralizer design that is mechanically similar to the hollow cathode design of the International Space Station Plasma Contactor. The ion optics assembly is similar to that of the NSTAR thruster, with an increased ion optics diameter to accommodate higher beam currents. It is in form-and-fit very close to the flight thruster and in function virtually identical to the flight thruster. In-depth descriptions of NEXT engine design and performance are detailed in Refs. [12-15].

A power console consisting of six commercially available power supplies and integrated recycle logic circuitry was used to energize the thruster. A high-purity xenon feed system delivered propellant to the discharge cathode, neutralizer cathode, and discharge chamber main through individual mass flow controllers. Tests were conducted in EP2 at The Aerospace Corporation. The cryogenically pumped facility is 2.4 meters in diameter and 10 meters in length, with a base pressure of 1.3×10^{-5} Pa (1.0×10^{-7} torr). The facility pressure, corrected for xenon, during TL28 operation is 3.6×10^{-4} Pa (2.7×10^{-6} torr). The NEXT thruster was installed in the facility directed toward a carbon beam stop mounted on the downstream endcap. A photograph of the thruster mounted in the facility is shown in Fig. 1. A data acquisition and control system utilizing commercial software was used to monitor ion engine operation. The acquisition system includes signal conditioners for the thruster currents and voltages, as well as commercial software that controls the input power to the thruster. Data was sampled at a frequency of 10-20 Hz, and the thruster currents, voltages, flow rates were written to a data file at a rate of 1 Hz during thruster operation.

Figure 1: NEXT engine mounted in EP2 for steady-state characterizations.

IV. Test Results

A. DART Performance Characterizations

NEXT engine performance and erosion characteristics were documented over a range of DART flow rates consistent with the desired flow control approach for the xenon flow system. Testing was confined to the beam voltage and beam current envelope highlighted in Fig. 2. The DART mission will be performed exclusively at a beam current of 2.70A, with a baseline beam voltage of V_b = 1021 V. The adjacent throttle levels may be used depending on the available input power to the propulsion system. In the following sections, the DTLXX-Y-Z nomenclature designates a DART throttle condition, complete with flow rates. The D denotes that the throttle level is DART-specific, Y indicates the total discharge chamber flow rate and Z designates the neutralizer flow rate. The highest flow rate is designated with an "A", "O" is the lowest, and "H" is the nominal flow. The nominal condition for the DART mission is DTL28-H-H. The flow splits that were investigated during testing are shown in Fig. 3. The full DART throttle table showing the set-point flows, currents, and voltages is in the Appendix.

	V_{bps}, V												
I_b, A	1800	1567	1396	1179	1021	936	850	700	679	650	400	300	275
3.52	TL40	TL39	TL38	TL37	ETL3.52A	ETL3.52B	ETL3.52C	ETL3.52D					
3.10	TL36	TL35	TL34	TL33	ETL3.1A	ETL3.1B	ETL3.1C	ETL3.1D	ETL3.1E				
2.70	TL32	TL31	TL30	TL29	TL28	ETL2.7A	ETL2.7B	ETL2.7C	ETL2.7D	ETL2.7E			
2.35	TL27	TL26	TL25	TL24	TL23	ETL2.35A	ETL2.35B	ETL2.35C	ETL2.35D	ETL2.35E			
2.00	TL22	TL21	TL20	TL19	TL18	ETL2.0A	ETL2.0B	ETL2.0C	ETL2.0D	ETL2.0E			
1.60	TL17	TL16	TL15	TL14	TL13	ETL1.6A	ETL1.6B	ETL1.6C	ETL1.6D	ETL1.6E	ETL1.6F		
1.20	TL12	TL11	TL10	TL09	TL08	TL07	TL06		TL05	TL04	TL03	TL02	
1.00													TL01

Figure 2: NEXT Throttle Table 11.1, with the highlighted region showing anticipated DART conditions.

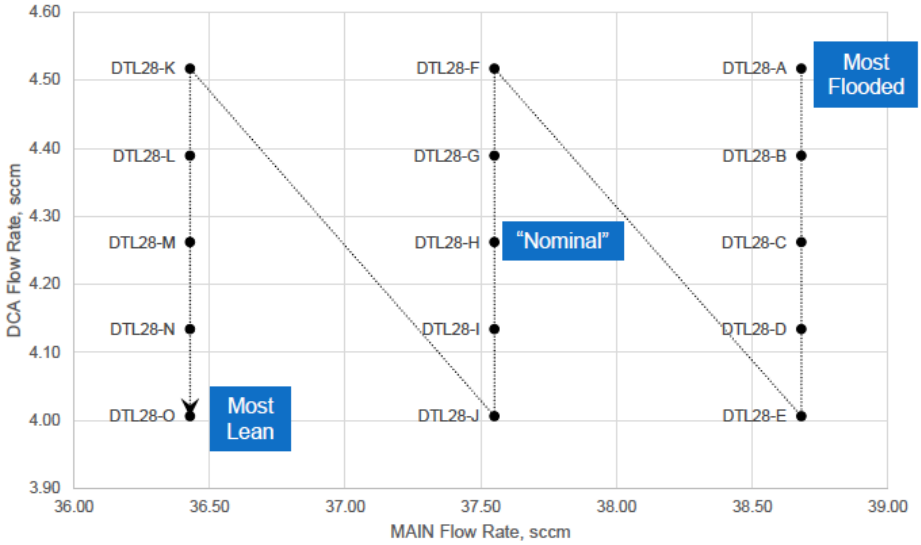

Figure 3: DART-specific flow sensitivity test matrix.

The divergence correction factor β and the doubly ionized thrust correction factor α were of particular interest during the testing campaign as they relate to the engine efficiency. In practice, β is determined from far-field beam current density measurements and α is calculated from mid-field charge state measurements. The charge state measurements are used to calculate the thruster efficiency, as well as the propellant utilization η_u:

$$\eta_u = \alpha \frac{J_b}{q} \frac{m_i}{\dot{m}_p} \tag{1}$$

The thrust T and the specific impulse I_{sp} are calculated from the propellant utilization efficiency and thrust correction factors through the relations:

$$T = \alpha\beta J_b \sqrt{\frac{2m_i V_b}{q}} \tag{2}$$

$$I_{sp} = \alpha\beta\eta_u \frac{1}{g} \sqrt{\frac{2m_i V_b}{q}} \tag{3}$$

The propellant utilization efficiency is shown in Fig. 4 for various propellant flow splits. The efficiency ranges from 0.871 – 0.931, with a value of 0.900 at the nominal condition of DTL28-H-H. While larger values of η_u can result in higher values of the specific impulse (and thruster efficiency), it can also lead to increased discharge ion energies as well as Xe^{++} production, both of which increase thruster internal erosion rates. The erosion products are a concern as they can redeposit within the thruster and cause electrical shorts, or they can migrate away from the thruster and interact with spacecraft surfaces. Several diagnostics were employed to characterize thruster erosion signatures – principally the erosion of molybdenum from the thruster ion optics accelerator electrode due to both direct-energetic ion erosion and charge-exchange ion erosion.

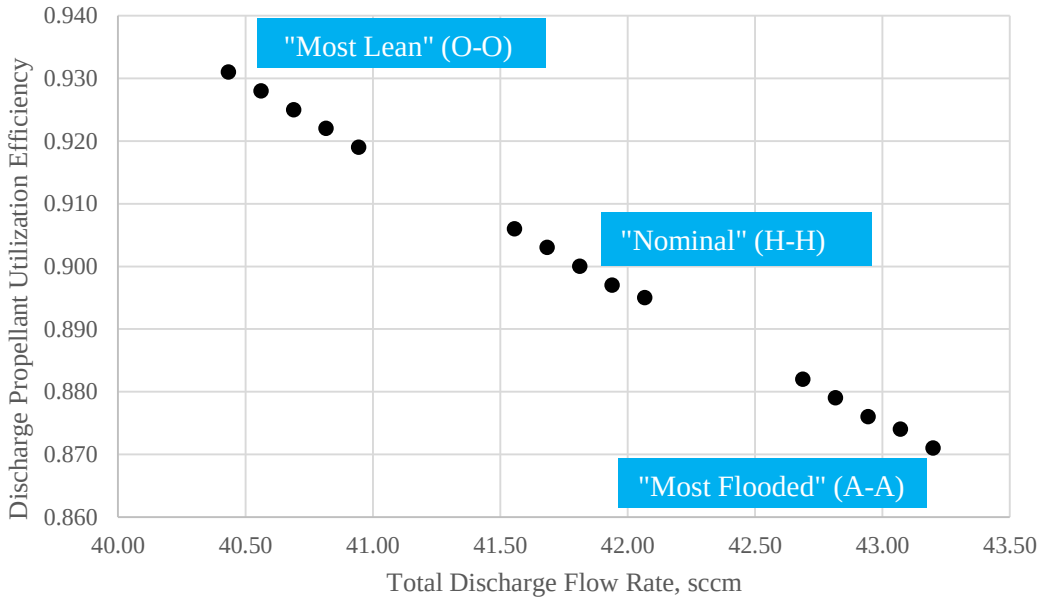

Figure 4: Propellant utilization efficiency for different flow variations.

Spatially-resolved NEXT thruster ion optics erosion measurements were made using LIF, and sputter-eroded erosion products from the thruster were documented at +/-36 degrees with respect to the exit plane of the engine thrust axis using a quartz crystal microbalance (QCM), over the range of DART operating conditions. A full description of the LIF test results is given in Ref. [11]. The key findings include:

a. QCM measurements and witness plates indicate higher grid material efflux than previous measurements documented on the NEXT thruster. The measurements indicate aperture barrel erosion (as opposed to downstream surface erosion) is the dominant mechanism, which may be expected over the first ~1000 hours of operation;

b. Changes in measured efflux accurately track the predicted behavior expected with variation in discharge flow rates: lean conditions yield reduced erosion, while flooded conditions increase erosion;

c. Worst-Case QCM analyses indicate << $1x10^{-11}$ gm/(cm^2-s) Mo mass deposition rates behind the exit plane of the thruster. These values were provided to APL for spacecraft plume modeling;

d. No anomalous erosion rates were found at any grid position or throttle level with LIF or QCM measurements, and there is substantial grid lifetime margin for the DART mission.

The singly to doubly ionized Xe ratio as a function of the total discharge flow rate is plotted in Fig 5. The variations in discharge flow rates results in a monotonic change in Xe^{++}/Xe^{+} with total discharge flow rate; it increases at lower total discharge flow rates (higher η_u and Isp); and decreases with higher total discharge flow rates (lower η_u and I_{sp}). This was expected from the trends in the discharge voltage as the flows were changed (Fig. 6). As stated earlier, the increased production of Xe^{++} ions can potentially lead to reduced thruster lifetimes. However, the combination of relatively low discharge voltages (< 30 V) and low Xe^{++} ion fractions indicate that erosion of cathode potential surfaces will not be an issue during the DART mission.

The divergence correction factor as a function of the total discharge flow rate is shown in Fig. 7. As expected, the relatively minor variations in propellant flow did not affect the plume divergence for a given throttle level. That is, for a given beam voltage, the plume divergence did not appreciably change as the flows were changed. The divergence modestly decreased with increasing beam voltage, which is consistent with prior plume measurements made with both EM and PM hardware.[16]

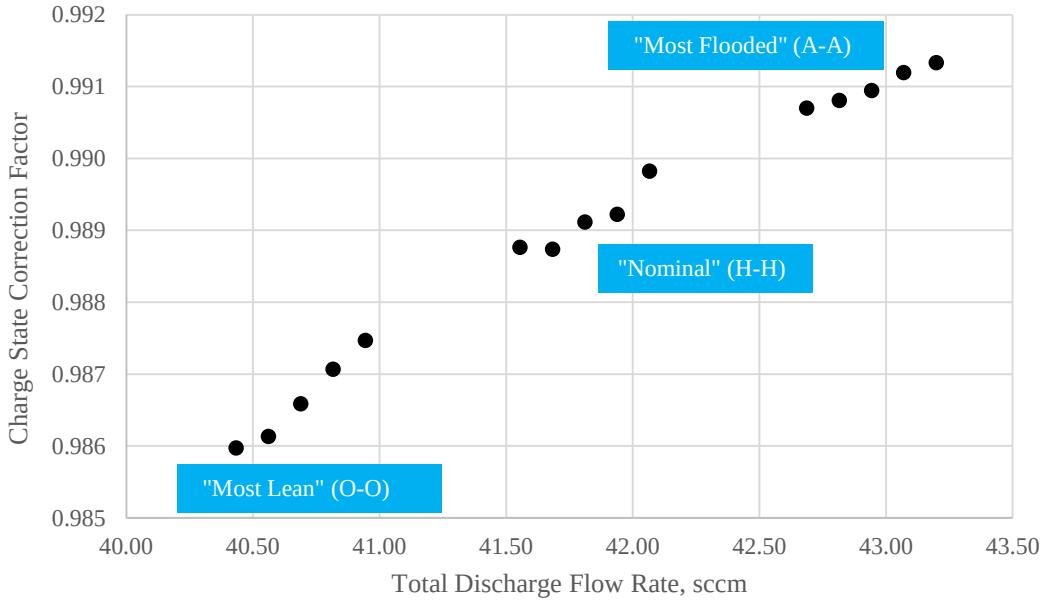

Figure 5: Thrust charge correction factor as a function of the total discharge flow rate.

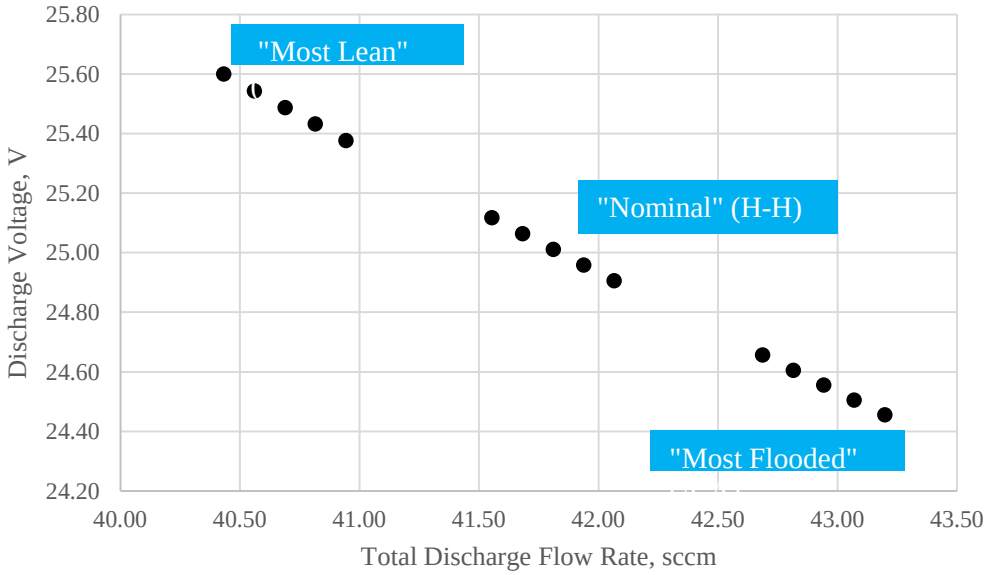

Figure 6: Discharge voltage as a function of the total discharge flow rate.

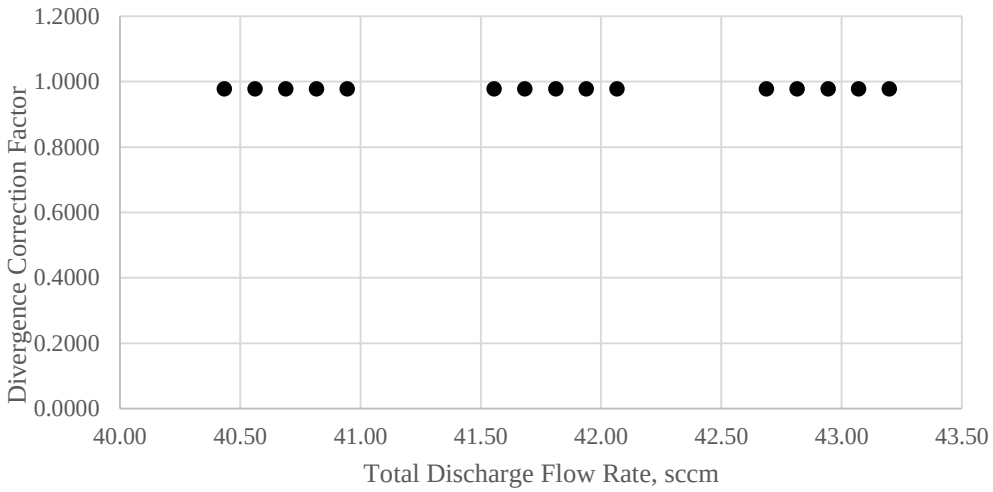

Figure 7: Divergence correction factor β as a function of total discharge flow rate.

The specific impulse and thruster efficiency for various propellant flow splits are shown in Figs. 8 and 9. The combined variations of Xe flow rates, and overall increase in neutralizer cathode assembly (NCA) flow rate leads to an I_{sp} range of 2,930 s – 3,140 s. The thruster efficiency values determined from α and β are consistent with data obtained from prior NEXT engine tests, and provide both a more-accurate and more-comprehensive assessment of performance at DART anticipated throttle conditions, given the XFS flow control approach.

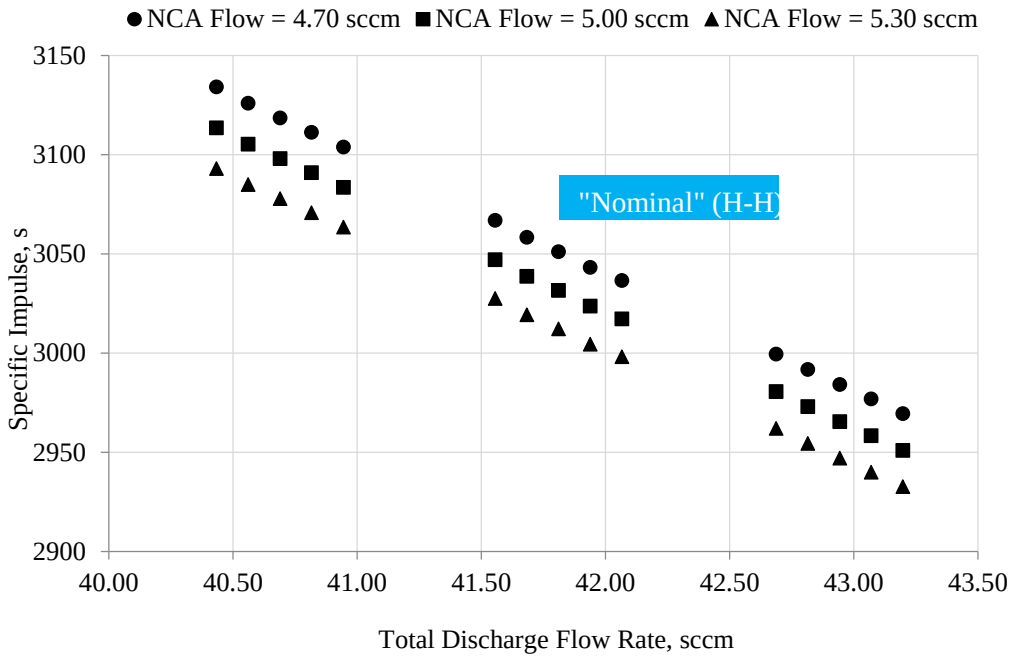

Figure 8: Specific impulse for lean, nominal, and flooded flow splits.

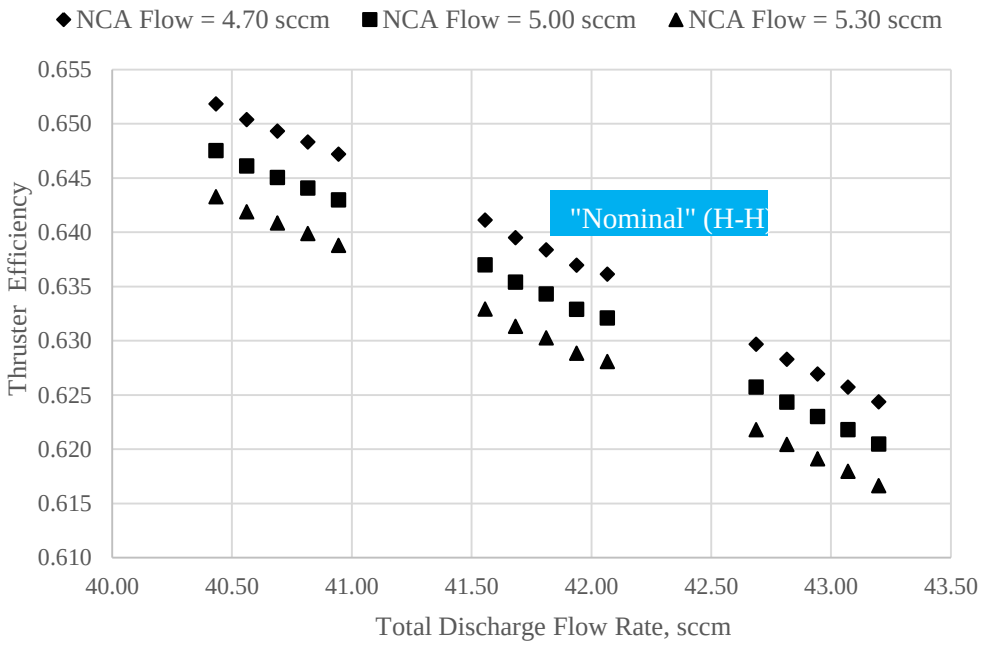

Figure 9: Thruster efficiency for lean, nominal, and flooded flow splits.

To summarize, NEXT thruster Xe ion plume was documented to characterize NEXT performance across all DART conditions and to provide validation data for modeling/simulation of the thruster plume. NEXT thruster operations are compatible with the proposed relaxation of flow control ranges for ignition and for steady-state operation. The relaxation in total discharge flow control increases the high-end discharge impedance leading to an increase in Xe^{++} production – although this should not be consequential for DART. Higher-than-nominal flow rates during steady-state operation did not significantly enhance charge-exchange erosion of the accelerator electrode as determined from LIF measurements.

B. Definition and Characterization of NEXT Operational Algorithms

Algorithms to operate the NEXT engine have been defined and tested as part of the NEXT-C project.[17-18] The algorithms were chosen to leverage the work that has been completed during the NEXT Phase II development effort, as well as the NSTAR flight projects. The algorithms include sequences to start the engine, regulate the beam current (thrust), and throttle across the entire throttle table. Given the limited performance envelope of the DART mission, the algorithms were revisited to investigate possible simplifications, and to ensure the sequences were consistent with DART CONOPS requirements. The algorithms that were characterized for the DART mission are as follows:

1. Cathode Conditioning: One-time procedure that is used to prepare thruster cathodes for operation after exposure to contaminating environments.

2. Discharge: Procedure for igniting the neutralizer cathode and then the discharge cathode.

3. Throttle: Procedure for igniting the thruster discharge, applying high voltage to the ion optics, and ramping the discharge current to achieve the set-point beam current.

4. Beam Current Regulation: Actively controls the beam current (thrust) during steady-state operation.

5. Power Throttling: Procedure for transitioning the engine to the desired throttle level during steady-state operation.

6. Shut Down: Procedure for removing input power and propellant flow from an operating thruster.

The Cathode Conditioning and Shutdown procedures from the NEXT-C project replicated those used in prior flight programs and were also adopted for DART. The Throttle and Beam Current Regulation sequences are described in the following paragraphs. While Power Throttling sequences were tested, they will not be utilized during the DART mission and will not be discussed further.

Multiple start-up sequences consistent with the DART CONOPS were defined and demonstrated by transitioning from an off-state to DTL28. The sequences captured a total of 9 separate throttle conditions, each at nominal, high, and low discharge and neutralizer flow rates. The typical 'cold' start-up thruster temperature was -30 C. A baseline start-up script was repeatedly demonstrated, yielding full-thrust operation in less than 8.0 minutes. The sequence incorporates a simultaneous heating of the cathode assemblies, followed by ignition of the neutralizer and discharge cathodes. This approach is a divergence from the standard NEXT-C startup procedure, but yields extremely-reliable ignition, and reduces the duration during which the PPU discharge power supply is energized open-circuit. Reliable neutralizer ignition was achieved at lean conditions vs. the NEXT-C specification, with rapid transition post ignition into quiescent spot-mode. No issues (e.g. thruster arcs, electron back-streaming) were encountered over dozens of thruster start-ups. Figure 10 shows the discharge voltage/current, beam current, accelerator current and coupling voltage during a start-up sequence. Time (t = 0) corresponds to the initiation of the sequence, that is, when current is applied to the cathode heaters. The discharge voltage V_d and coupling voltage V_g stay within nominal NEXT operating ranges, and reach steady-state values within minutes of high voltage application. The peak ('hump') in accelerator current J_a is likely due to improper steering of the discharge plasma; as the beam current is increased the ions are properly focused through the apertures yielding decreased impingement currents. The peak accelerator current (~ 14 mA) is of short duration and is within the bounds of typical NEXT operation—minimizing any related lifetime concerns. The discharge J_d and beam currents J_b are discussed further below.

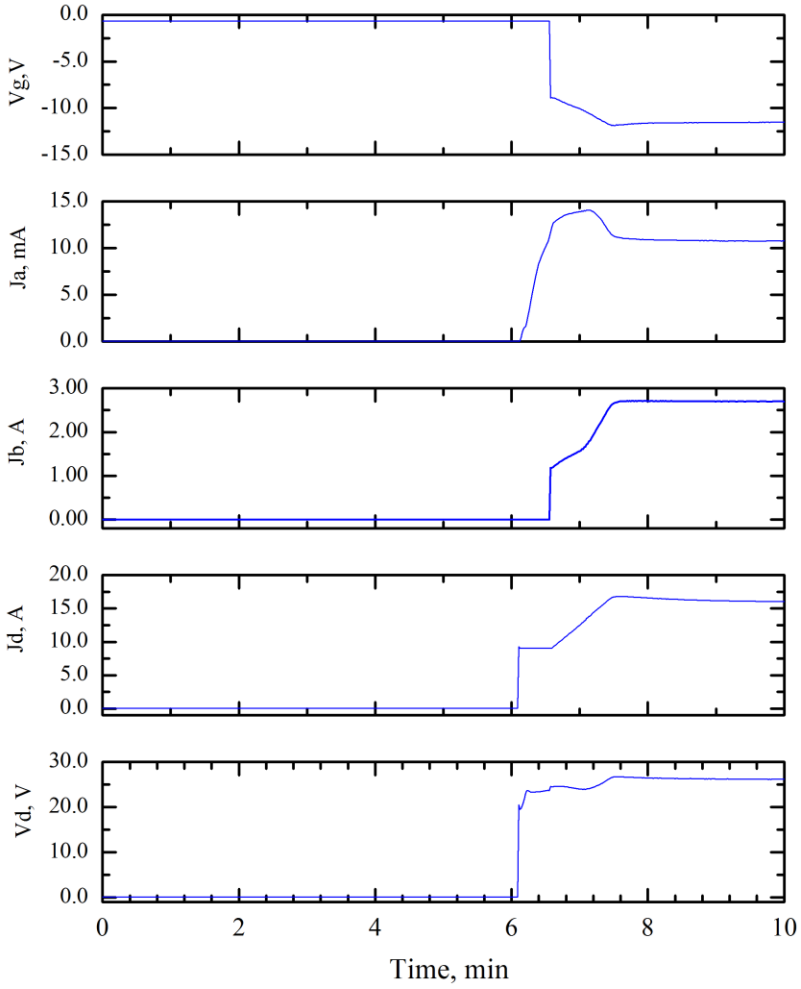

Figure 10: Thruster telemetry during a typical automated start-up.

A typical thrust vector measurement obtained during start-up is shown in Fig. 11. The thrust vector is defined as the beam centroid offset angle (as measured by a rake of Faraday probes 1 m from the thruster exit plane) from the center-line of the thruster. Qualitatively, the time-resolved behavior of the thrust vector tracks the changes in the electrode grid gap as the thruster heats up. The thrust vector measurements and analyses were provided to the APL Guidance, Navigation, and Control team, and influenced the final design of the NEXT-C diagnostic package that will be employed to characterize the flight thrusters.

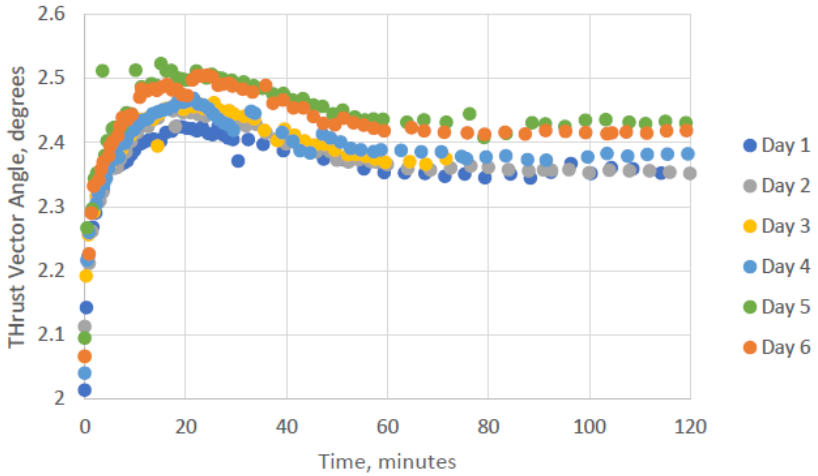

Figure 11: Thrust vector off-set angle during start-ups at DART conditions (t = 0 corresponds to the application of HV).

The beam current regulation algorithm is used to control the beam current and maintain constant thrust during steady-state operation. The algorithm operates through closed-loop control of the discharge current. When the true beam current differs from the set-point value (as specified in the lookup table), the discharge current is changed by the amount that the beam current is in error, to a specified limit. The adjustment limit was variable during the testing, and the baseline value was based on a direct scaling from the NSTAR engine. The algorithm operates with a sampling rate of 1 Hz. Minimum beam current and beam stability criteria are incorporated into the algorithm to prevent regulation during transient arc events. A zoom-in of the beam current during a typical start-up is shown in Fig. 12. During a thruster start-up, the discharge is ignited at the set-point value and the beam current regulation algorithm increases the discharge current until the set-point beam current of 2.70 is reached. More than two-dozen automated sequences were executed, both under 'cold' (-30 C) and 'hot' (+30 C) conditions, exercising the Throttle, Beam Current Regulation, Power Throttling, and Shutdown algorithms. Each sequence consisted of a thruster start-up, a ~2 hour burn at steady-state using Beam Current regulation (constant thrust), a Power-Throttling sequence using an algorithm to increase and decrease thruster input power (changing the power order each time, up-down, down-up), followed by a shutdown. The time required to start the engine and ramp to the set-point power level was found to be highly repeatable and the thrust was regulated to well within 1% during steady-state operation for all DART conditions.

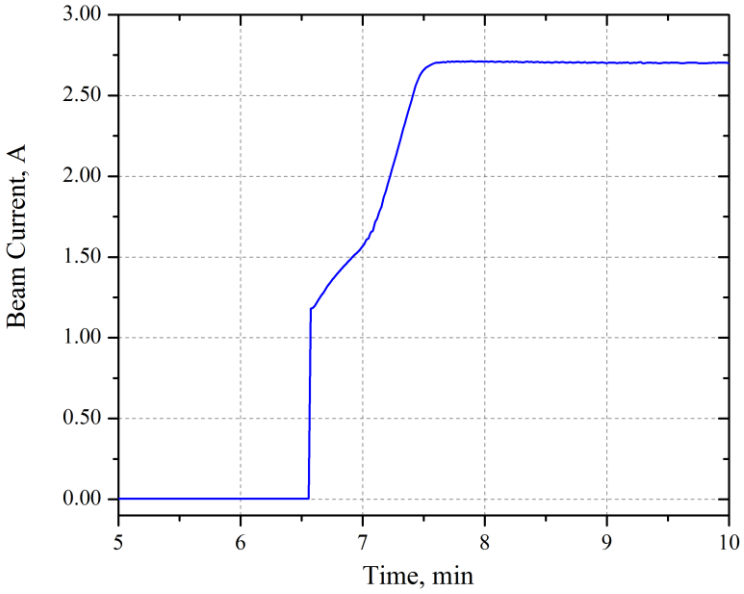

Figure 12: Beam current response during a typical startup sequence.

V. Summary

Steady-state performance, lifetime and erosion, and flow sensitivity data have been successfully obtained at anticipated DART operating conditions. Thrust correction factors and propellant efficiency data were used to refine the thruster performance database at anticipated DART operating conditions. It was found that the relaxation in the discharge flow control increases the high-end discharge impedance and the production of Xe^{++} ions, although the increases are modest and inconsequential for DART. Similarly, operating at 'flooded' discharge flow rates was found to increase the erosion of the accelerator electrode due to increased charge-exchange collisions, although this increase is of no consequence for DART given the modest throughput required for the mission. Higher-than-nominal neutralizer flow rate during steady-state operation does not deleteriously impact neutralizer operation, nor significantly enhance charge-exchange erosion of the accelerator electrode. The sputter-eroded efflux from the thruster was documented forward-and-behind the exit plane of the thruster over a range of DART throttle conditions, and was provided to APL for plume modeling analysis. A baseline start-up script was defined and repeatedly demonstrated from ambient (-30 C) to full-power for DART, yielding full-thrust operation in less than 7.0 minutes. Thrust vector and thrust vector stability has been characterized at start-up and through thermal equilibrium. Algorithms were defined, developed, and validated repeatedly under a variety of thermal conditions encompassing the anticipated DART Mission conditions. No issues were encountered during the algorithm tests, and the beam current regulation algorithm controlled the thrust to less than 1%, which is well within the mission requirement. NEXT thruster operations are compatible with the proposed relaxation of flow control ranges for ignition and for steady-state operation.

Appendix: DART Specific Throttle Table

Throttle Level	Beam Current, A	Beam Voltage, V	Accel. Voltage, V	Main Flow, sccm	Cath. Flow, sccm	Neut. Flow, sccm
DETL2.7B-A-A	2.700	936	-175	38.682	4.517	5.300
DETL2.7B-H-A	2.700	936	-175	37.550	4.262	5.300
DETL2.7B-O-A	2.700	936	-175	36.428	4.006	5.300
DETL2.7B-A-H	2.700	936	-175	38.682	4.517	5.000
DETL2.7B-H-H	2.700	936	-175	37.550	4.262	5.000
DETL2.7B-O-H	2.700	936	-175	36.428	4.006	5.000
DETL2.7B-A-O	2.700	936	-175	38.682	4.517	4.700
DETL2.7B-H-O	2.700	936	-175	37.550	4.262	4.700
DETL2.7B-O-O	2.700	936	-175	36.428	4.006	4.700
DTL28-A-A	2.700	1021	-175	38.682	4.517	5.300
DTL28-H-A	2.700	1021	-175	37.550	4.262	5.300
DTL28-O-A	2.700	1021	-175	36.428	4.006	5.300
DTL28-A-H	2.700	1021	-175	38.682	4.517	5.000
DTL28-H-H	2.700	1021	-175	37.550	4.262	5.000
DTL28-O-H	2.700	1021	-175	36.428	4.006	5.000
DTL28-A-O	2.700	1021	-175	38.682	4.517	4.700
DTL28-H-O	2.700	1021	-175	37.550	4.262	4.700
DTL28-O-O	2.700	1021	-175	36.428	4.006	4.700
DTL29-A-A	2.700	1179	-200	38.682	4.517	5.300
DTL29-H-A	2.700	1179	-200	37.550	4.262	5.300
DTL29-O-A	2.700	1179	-200	36.428	4.006	5.300
DTL29-A-H	2.700	1179	-200	38.682	4.517	5.000
DTL29-H-H	2.700	1179	-200	37.550	4.262	5.000
DTL29-O-H	2.700	1179	-200	36.428	4.006	5.000
DTL29-A-O	2.700	1179	-200	38.682	4.517	4.700
DTL29-H-O	2.700	1179	-200	37.550	4.262	4.700
DTL29-O-O	2.700	1179	-200	36.428	4.006	4.700

References

[1] Patterson, M., Foster, J., Haag, T., Rawlin V., Soulas, G., Roman, R., "NEXT: NASA's Evolutionary Xenon Thruster," *38th AIAA/ASME/SAE/ASEE Joint Propulsion Conference & Exhibit*, Indianapolis, IN, AIAA-2002-3832.

[2] Oleson, S., Gefert, L., Sims, J., Noca, M., Patterson, M., and Benson, S., "Mission Advantages of NEXT: NASA's Evolutionary Xenon Thruster," *38th AIAA/ASME/SAE/ASEE Joint Propulsion Conference & Exhibit*, Indianapolis, IN, AIAA-2002-3969.

[3] Soulas, G., Patterson, M., Pinero, L., Herman, D., and Snyder, J., "NEXT Single String Integration Test Results," *45th AIAA/ASME/SAE/ASEE Joint Propulsion Conference & Exhibit*, Denver, CO, AIAA-2009-4816.

[4] Patterson, M., Foster, J., McEwen, H., Herman, D., Pencil, E., and VanNoord, J., "NEXT Multi-Thruster Array Test - Engineering Demonstration," *42nd AIAA/ASME/SAE/ASEE Joint Propulsion Conference & Exhibit*, Sacramento, CA, AIAA-2006-5180.

[5] Snyder, J.S., Anderson, J.R., VanNoord, J.L., and Soulas, G.C., "Environmental Testing of the NEXT PM1R Ion Engine," *30th International Electric Propulsion Conference*, Florence, Italy, IEPC-2007-276.

[6] Soulas, G., Domonkos, M., and Patterson, M., "Wear Test Results for the NEXT Ion Engine," *39th AIAA/ASME/SAE/ASEE Joint Propulsion Conference and Exhibit*," Huntsville, AL, AIAA-2003-4863.

[7] Shastry, R., Herman, D.A., Soulas, G.C., and Patterson, M.J., "End-of-test Performance and Wear Characterization of NASA's Evolutionary Xenon Thruster (NEXT) Long-Duration Test," *50th AIAA/ASME/SAE/ASEE Joint Propulsion Conferenc*e, Cleveland, OH, AIAA-2014-3617.

[8] Fisher, J., Ferriauolo, B., Hertel, T., Monheiser, J., Barlog, C., Allen, M., Myers, R., Hoskins, A., Bontempo, J., Nazario, M., Shastry, R., Soulas, G., and Aulisio, M., "NEXT-C Flight Ion Propulsion Development Status," *35th International Electric Propulsion Conference*, Atlanta, GA, IEPC-2017-218.

[9] Shastry, R., Soulas, G., Aulisio, M., and Schmidt, G., "Current Status of NASA's NEXT-C Ion Propulsion System Development Project," *68th International Astronautical Congress*, Adelaide, Australia, IAC-17.C4.4.3.

[10] Young, J.A., Matlock, T., Nakles, M., Crofton, M.W., Patterson, M.J., Arthur, N.A., and John, J., "Far Field Plume Distribution and Divergence for NEXT: DART Mission," *AIAA Scitech 2019 Forum*, Orlando, FL, AIAA-2019-1243.

[11] Crofton, M.W., Schoeffler, D., Young, J.A., Patterson, M.J., and John, J., "LIF Erosion Rate Measurements of NEXT Ion Engine for DART Mission," *AIAA Scitech 2019 Forum*, Orlando, FL, AIAA-2019-1246.

[12] Hoskins, A., Wilson, F., Patterson, M., Soulas, G., Polaha, J., Talerico, L., "Development of a Prototype Model Ion Thruster for the NEXT System," *40th AIAA/ASME/SAE/ASEE Joint Propulsion Conference and Exhibit*, Fort Lauderdale, FL, AIAA-2004-4111.

[13] Soulas, G., Domonkos, M., and Patterson, M., "Performance Evaluation of the Next Ion Engine," 39*th AIAA/ASME/SAE/ASEE Joint Propulsion Conference and Exhibit*, Hunstville, AL, AIAA-2003-5278.

[14] Herman, D., Soulas, G., Patterson, M., "Performance Evaluation of the Prototype-Model NEXT Ion Thruster," *43rd AIAA/ASME/SAE/ASEE Joint Propulsion Conference & Exhibit*, Cincinnati, OH, AIAA-2007-5212.

[15] Diamant, K., Pollard, J., Crofton, M., Patterson, M., and Soulas, G., "Thrust Stand Characterization of the NASA NEXT Thruster," *46th AIAA/ASME/SAE/ASEE Joint Propulsion Conference & Exhibit*, Nashville, TN, AIAA-2010-6701.

[16] Pollard, J.E., Diamant, K.D., Crofton, M.W., Patterson, M.J., and Soulas, G.c., "Spatially-Resolved Beam Current and Charge State Distributions for the NEXT Ion Engine," *46th AIAA/ASME/SAE/ASEE Joint Propulsion Conference & Exhibit*, Nashville, TN, AIAA-2010-6779.

[17] Thomas, R.E., Patterson, M.J., Soulas, G.C., "Development and Validation of Autonomous Operational Sequences for the NEXT Ion Propulsion System," 52*th AIAA/ASME/SAE/ASEE Joint Propulsion Conference & Exhibit*, Salt Lake City, UT, AIAA-2016-5077.

[18] Thomas, R.E., Patterson, M.J., and Soulas, G.C., "Algorithm Validation Testing of the NEXT Ion Propulsion System," *63rd Joint Army-Navy-NASA-Air Force Propulsion Meeting*, Newport News, VA, 2016.